

1

Measurement and Proper Equalization of Range Sidelobes Using a Spherical Satellite as a Reflector

By

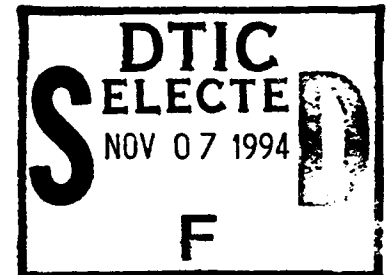
A. G. Kramer

August 1994

Prepared for

Program Director
Surveillance and Control Systems
Electronic Systems Center
Air Force Materiel Command
United States Air Force

Hanscom Air Force Base, Massachusetts



AD-A285 955

309

94-34434



DTIC QUALITY INSPECTED 5

Project No. 5830

Prepared by

The MITRE Corporation
Bedford, Massachusetts

Contract No. F19628-94-C-0001

Approved for public release;
distribution unlimited.

94 11 4 080

When U.S. Government drawings, specifications or other data are used for any purpose other than a definitely related government procurement operation, the government thereby incurs no responsibility nor any obligation whatsoever; and the fact that the government may have formulated, furnished, or in any way supplied the said drawings, specifications, or other data is not to be regarded by implication or otherwise as in any manner licensing the holder or any other person or conveying any rights or permission to manufacture, use, or sell any patented invention that may in any way be related thereto.

Do not return this copy. Retain or destroy.

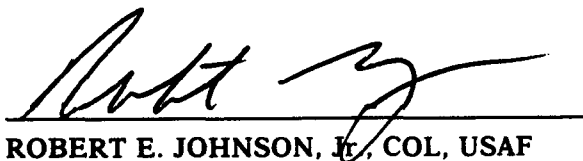
REVIEW AND APPROVAL

This technical report has been reviewed and is approved for publication.



M. RAY NEAL, CAPT, USAF
Program Manager, EWR
Surveillance and Control Systems

FOR THE COMMANDER



ROBERT E. JOHNSON, JR., COL, USAF
Program Director
Surveillance and Control Systems

REPORT DOCUMENTATION PAGE

Form Approved
OMB No. 0704-0188

Public reporting burden for this collection of information is estimated to average 1 hour per response, including the time for reviewing instructions, searching existing data sources, gathering and maintaining the data needed, and completing and reviewing the collection of information. Send comments regarding this burden estimate or any other aspect of this collection of information, including suggestions for reducing this burden, to Washington Headquarters Services, Directorate for Information Operations and Reports, 1215 Jefferson Davis Highway, Suite 1204, Arlington, VA 22202-4302, and to the Office of Management and Budget, Paperwork Reduction Project (0704-0188), Washington, DC 20503.

| | | | | |
|---|---|--|--|--|
| 1. AGENCY USE ONLY (Leave blank) | | 2. REPORT DATE August 1994 | 3. REPORT TYPE AND DATES COVERED Final | |
| 4. TITLE AND SUBTITLE Measurement and Proper Equalization of Range Sidelobes Using a Spherical Satellite as a Reflector | | | 5. FUNDING NUMBERS F19628-94-0001 5830 | |
| 6. AUTHOR(S) Kramer, A. G. | | | | |
| 7. PERFORMING ORGANIZATION NAME(S) AND ADDRESS(ES) The MITRE Corporation 202 Burlington Road Bedford, MA 01730 | | | 8. PERFORMING ORGANIZATION REPORT NUMBER MTR 11162 | |
| 9. SPONSORING/MONITORING AGENCY NAME(S) AND ADDRESS(ES) Director, Surveillance and Control Systems (ESC/TNB) Electronic Systems Center, AFMC 5 Eglin Street Hanscom AFB, MA 01731-2121 | | | 10. SPONSORING/MONITORING AGENCY REPORT NUMBER ESC-TR-94-196 | |
| 11. SUPPLEMENTARY NOTES | | | | |
| 12a. DISTRIBUTION/AVAILABILITY STATEMENT Approved for public release; distribution unlimited | | | 12b. DISTRIBUTION CODE | |
| 13. ABSTRACT (Maximum 200 words) We have investigated the problems of measuring range sidelobes by using a small sphere (ka 15) as a target. This measurement scheme requires coherent integration to increase the signal-to-noise ratio at the sidelobes to a level where accurate estimation is possible. We determined that two pathologic coherent responses can occur in this situation. A wave creeping around the sphere causes the formation of an asymmetric range sidelobe that lags the main response. We find that the relative level of coherent errors, whose magnitude is below the noise on a single pulse basis, is invariant with coherent integration. | | | | |
| 14. SUBJECT TERMS range sidelobes creeping waves signal-to-noise ratio | | | 15. NUMBER OF PAGES 31 | |
| | | | 16. PRICE CODE | |
| 17. SECURITY CLASSIFICATION OF REPORT Unclassified | 18. SECURITY CLASSIFICATION OF THIS PAGE Unclassified | 19. SECURITY CLASSIFICATION OF ABSTRACT Unclassified | 20. LIMITATION OF ABSTRACT SAR | |

ACKNOWLEDGMENTS

This document has been prepared by MITRE Corporation under Project No. 5830, Contract No. F19628-94-C-0001. The contract is sponsored by the Electronic Systems Center, Air Force Materiel Command, United States Air Force, Hanscom Air Force Base, Massachusetts 01731-3010.

| | |
|--------------------|-------------------------------------|
| Accession For | |
| NTIS CRA&I | <input checked="" type="checkbox"/> |
| DTIC TAB | <input type="checkbox"/> |
| Unannounced | <input type="checkbox"/> |
| Justification | |
| By | |
| Distribution/ | |
| Availability Codes | |
| Dist | Avail and/or Special |
| A-1 | |

TABLE OF CONTENTS

| SECTION | PAGE |
|------------------------|------|
| 1 Introduction | 1 |
| 2 Range Sidelobes | 3 |
| 3 Error Effects | 7 |
| 4 Measurement | 9 |
| 5 Pathologic Phenomena | 11 |
| 6 Correct Approach | 21 |
| 7 Conclusions | 23 |
| List of References | 25 |
| Bibliography | 27 |
| Appendix A | A-1 |

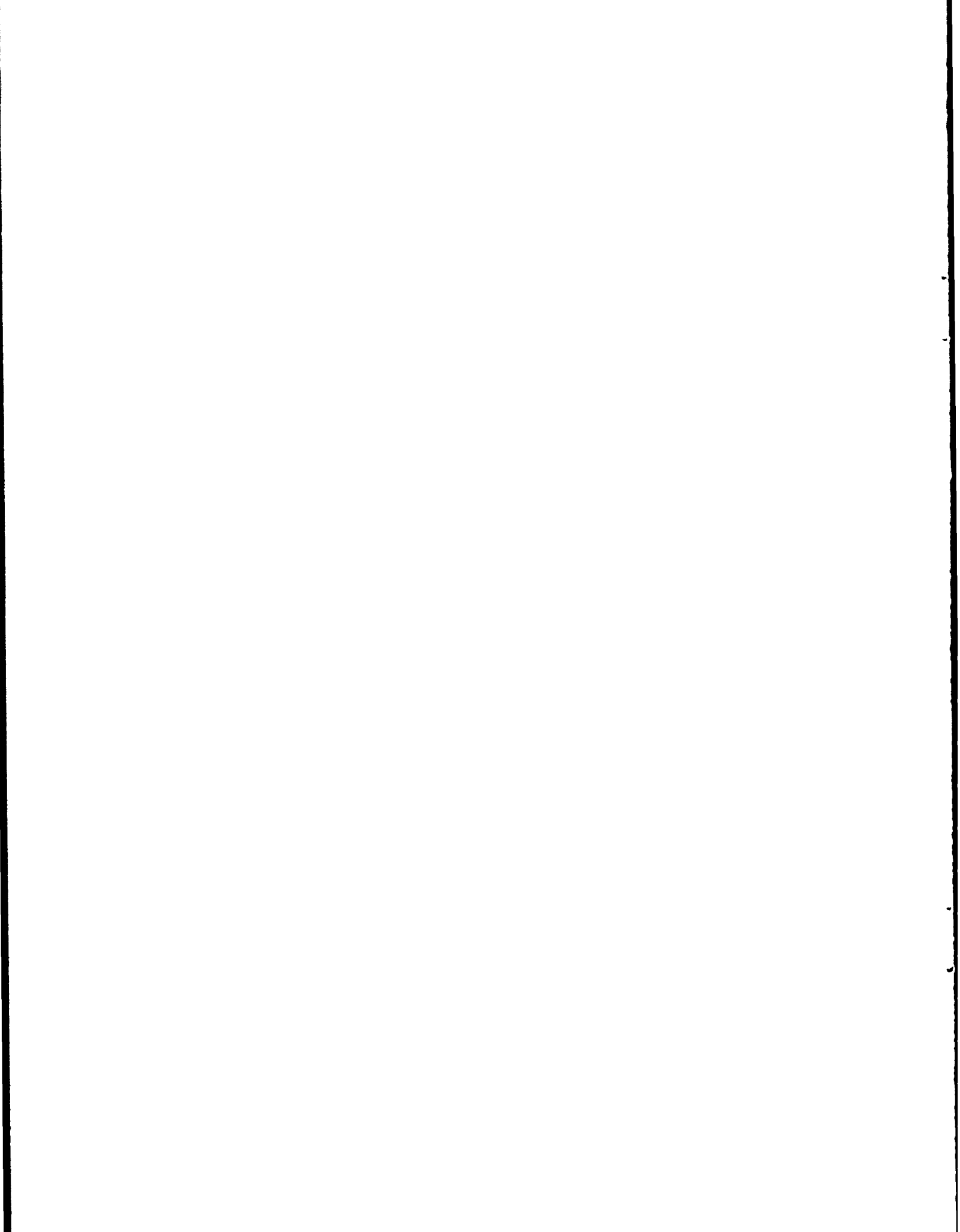
LIST OF FIGURES

| FIGURE | PAGE |
|--|------|
| 2-1 Uniformly Weighted Compressed Pulse | 4 |
| 2-2 Taylor Weighting ($\bar{n} = 7$, Sidelobe Level = 42 dB) | 5 |
| 2-3 Taylor Weighted ($\bar{n} = 7$, Sidelobe Level = 42 dB) Time Pulse | 6 |
| 5-1 Radar Cross Section of 5398 in the High Resolution Operating CDSM Band | 14 |
| 5-2 Schematic View of Reflection from a Conducting Sphere | 15 |
| 5-3 Time Waveforms | 17 |
| 5-4 Equalization Network | 18 |
| 5-5 Equalized and Unequalized Waveforms | 19 |
| 5-6 Radar Returns from Two Adjacent Targets | 20 |

SECTION 1

INTRODUCTION

The COBRA DANE System Modernization Program (CDSM) will effect improvements in the performance of the COBRA DANE (AN/FPS-108) radar. The CDSM replaces obsolescent hardware, including the receiver-exciter, the signal processor and post processor, and the automatic data processing equipment. The current software will be replaced with a structured program written in Ada. The CDSM will incorporate improved performance requirements. In particular, the range sidelobe requirements on the compressed medium and high resolution waveforms are increased to 27 dB below the main lobe for high resolution and 35 dB below the main lobe for medium resolution. This paper discusses range sidelobes, their origin and measurement, and several measurement-related pathologic phenomena that should be avoided.



SECTION 2

RANGE SIDELOBES

We consider a constant amplitude linear FM waveform of bandwidth B and pulse-length T , as shown in equation 2.1.

$$F(t) = \exp\left\{j\frac{\pi Bt^2}{T}\right\} \quad \left(|t| \leq \frac{T}{2}\right) \quad (2.1)$$

where $j = \sqrt{-1}$. In the frequency domain, we approximate the spectrum, for large values of the BT product, as

$$G(v) = \exp\left\{-j\frac{\pi Tv^2}{B}\right\} \quad \left(|v| \leq \frac{B}{2}\right) \quad (2.2)$$

If we multiply the frequency domain waveform of equation 2.2 by its complex conjugate to remove the frequency modulation -- the dechirping process -- and transform the resultant waveform to the time domain, we get the compressed pulse shown in equation 2.3.

$$F'(t) = \frac{\sin \pi Bt}{\pi Bt} = \text{sinc } \pi Bt \quad (2.3)$$

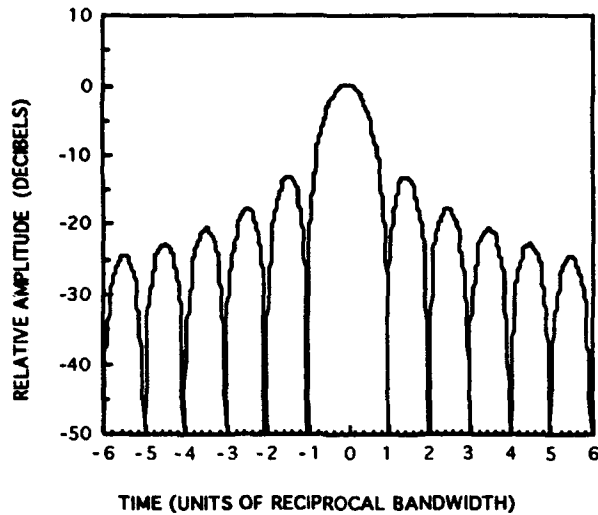


Figure 2-1. Uniformly Weighted Compressed Pulse

The compressed pulse shown in figure 2-1 has a first sidelobe that is about 13 dB below the main lobe peak. We can reduce the magnitude of the sidelobes with respect to the main lobe by appropriately weighting the amplitude of the frequency response. Typically, we use T.T. Taylor weighting, characterized by two numbers, \bar{n} and SLL, where \bar{n} is the number of constant amplitude sidelobes which are SLL (in decibels) below the main lobe. The relationship between \bar{n} , SLL, and the Taylor weighting function F_T is shown in appendix A. Figure 2-2 shows the Taylor weighting function for the case $\bar{n} = 7$ and SLL = 42 dB.

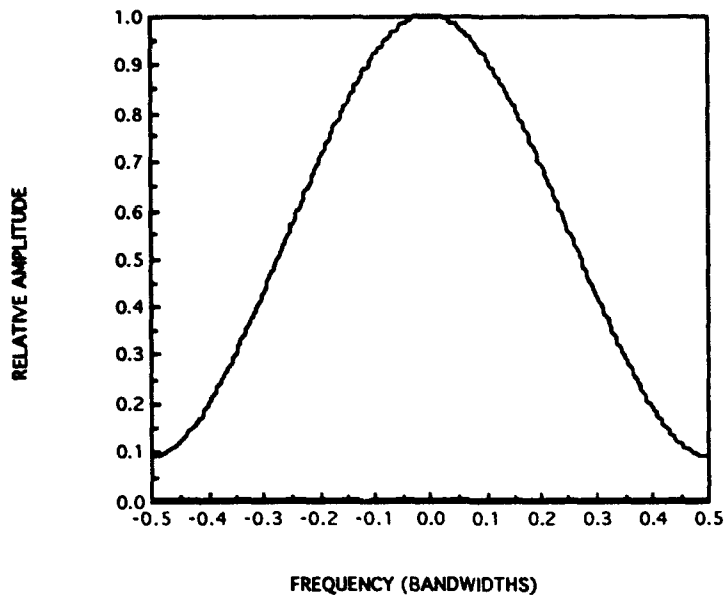


Figure 2-2. Taylor Weighting ($\bar{n} = 7$, Sidelobe Level = 42 dB)

The compressed time pulse is the Fourier transform of the weighting function. The relationship in equation 2.4 determines the shape of the time domain pulse.

$$F_T(t) = \left[1 + 2 \sum_{m=1}^{\bar{n}-1} \frac{(-1)^m F_m (Bt)^2}{(Bt)^2 - m^2} \right] \text{sinc } \pi Bt \quad (2.4)$$

We derive the relationship between \bar{n} , SLL, and the weighting coefficients, F_m , in appendix A. Figure 2-3 shows the shape of the pulse $F_T(t)$ as a function of time (plotted using a decibel scale).

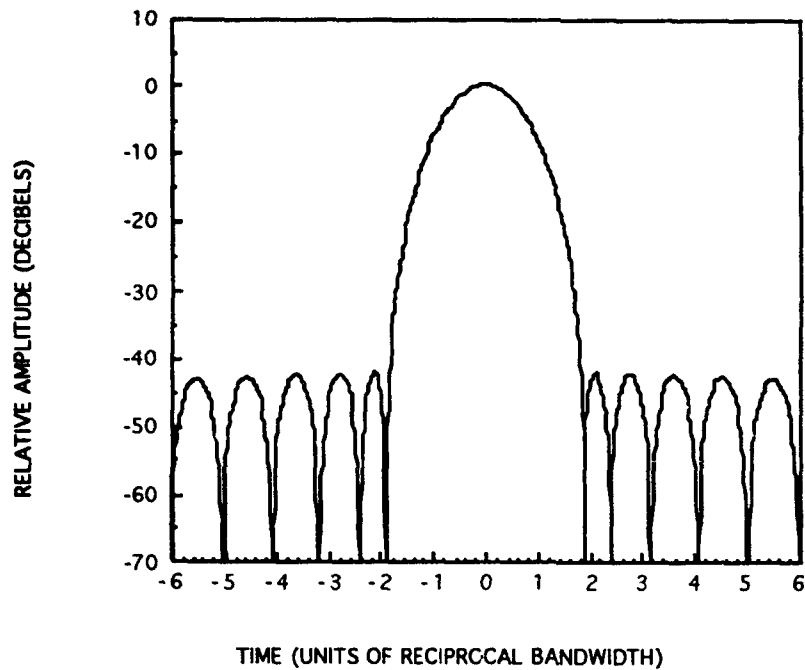


Figure 2-3. Taylor Weighted ($\bar{n} = 7$, Sidelobe Level = 42 dB) Time Pulse

The compressed pulse with Taylor weighting has significantly lower sidelobes than the uniformly weighted pulse. However, the width of the Taylor weighted pulse, measured at any level below the peak, is greater than the corresponding width of the uniformly weighted pulse.

SECTION 3

ERROR EFFECTS

The mathematical analysis in section 2 assumes that an idealized radar is used for transmission and reception. In practice, the received signal is accompanied by phase and amplitude errors in the transfer function of the hardware, through which the signal passes. Range sidelobe levels are degraded by mismatches and fluctuations in any hardware through which it passes. The effect of each of the individual hardware blocks are assumed to be independent so the total noise power, N_T , is the sum of each of the individual component error noise, N , plus the thermal noise N_0 . Since the total number of noise sources is large, the distribution of the resultant total noise is approximately Gaussian. The distribution of the amplitude of the signal i.e., the design sidelobe level S_d , plus noise (R), is Ricean. The probability of R lying between R and $R + dR$ is

$$p(R) dR = \frac{R dR}{N_T} \exp\left(-\frac{R^2 + S_d^2}{2N_T}\right) I_0\left(\frac{RS_d}{N_T}\right) dR \quad (3.1)$$

where I_0 is the modified Bessel function of the first kind of order 0. Then, the confidence of achieving a given sidelobe power level, $\frac{R^2}{2}$, is

$$C_s(a,b) = \int_0^b \left\{ \exp\left(-\frac{a^2 + v^2}{2}\right) \right\} I_0(av) v dv \quad (3.2)$$

where $a = \frac{S_d}{\sqrt{N_T}}$ and $b = \frac{R}{\sqrt{N_T}}$. The confidence integral C_s of equation 3.1 is related to the Q function defined by Marcum^[1] by the relationship

$$C_s(a,b) = 1 - Q(a,b) \quad (3.3)$$

The Q function is tabulated in the literature^[2].

Coherent integration can be used in the measurement process to reduce the effect of thermal noise and noise-like errors. That is, if M pulses are coherently integrated, the effective noise is reduced by a factor of M and thus

$$a_M = a\sqrt{M}; \quad b_M = b\sqrt{M} \quad (3.4)$$

SECTION 4 MEASUREMENT

Ideally, we should measure the range sidelobe level for a given waveform on a single pulse basis. We structured the system specification for the COBRA DANE System Modernization (CDSM) program to require range sidelobes to be defined for a single pulse. The measurement should include all of the components of the radar system that contribute to waveform degradation. These include the exciter, transmitter, antenna, receiver, and signal processor. The measurement also requires the transmitted signal to reflect from a target that lies in the Fraunhofer region of the antenna. The measurement must use a suitable target located at a known range, have a radar cross section (RCS) that is time invariant, and have an RCS that ensures the signal-to-noise ratio is large enough for the measurement to be accurate. The range sidelobe must be above the system noise level.

We derive the required signal-to-noise ratio for a given measurement accuracy (1σ) in the following manner. Equation 4.1 shows the relationship between the standard deviation, σ_A , of the error of an amplitude measurement normalized to the true value of the measured quantity, $\frac{\delta A}{A}$, and the signal-to-noise ratio, $\frac{S}{N}$.

$$\sigma_A = \frac{\delta A}{A} = \frac{1}{\sqrt{\frac{2S}{N}}} \quad (4.1)$$

We find the the 1σ error in decibels, ϵ_A , from the relationship in equation 4.2.

$$(1 + \sigma_A)^2 = 10^{0.10\epsilon_A} \quad (4.2)$$

For a measurement standard deviation of 1 dB (1 dB accuracy), the required signal-to-noise ratio is 15.26 dB. If the sidelobe level is γ dB below the main lobe of the compressed waveform, then the required signal-to-noise ratio at the peak of the main lobe is $\gamma + \epsilon_A$ dB. Thus, we require a signal-to-noise ratio of 50.3 dB at the peak of the compressed weighted pulse in order to measure the 35 dB range sidelobes specified for the CDSM to 1 dB accuracy.

We prefer to use a target whose return is time invariant. A spherical reflector conforms to this requirement. In the ideal case, a large sphere that gives a return with a signal-to-noise ratio greater than 50.3 dB is preferred. However, such a large spherical target does not exist in the satellite catalog. If the sphere is located at a slant range of 1000 nmi from COBRA DANE, we find the required RCS, σ_T , in decibels with respect to one square meter (dBsm) from equation 4.3

$$\sigma_T = 50.3 + 10 \log_{10} \left(\frac{1000}{\tau} \right) - (S_{CD} + 20) \quad (4.3)$$

where S_{CD} is the specified CDSM sensitivity of 12.0 dB for a target of -20 dBsm RCS illuminated with a 1000 microsecond pulse, and τ is the radar pulse length used. Thus, if we use a pulse whose length is 125 microseconds, we must utilize a sphere whose RCS is 27.3 dBsm for an accurate single pulse measurement. The satellite catalog does not contain a sphere that large. Consequently, we are forced to utilize coherent integration of returns from small spheres.

SECTION 5

PATHOLOGIC PHENOMENA

We define a small sphere as one whose equatorial circumference, ka (a the wave number), is less than 50 wavelengths. We express the quantity ka as, $ka = \frac{2\pi a}{\lambda}$, where a is the radius of the sphere and λ is the operating wavelength. Measurements taken with small RCS spheres in conjunction with coherent integration of data are vulnerable to two pathologic phenomena: coherent errors and creeping wave effects.

Not all error terms are noise-like; thus they are incoherent from pulse to pulse. Coherent interference can be present that will affect the range sidelobes. For example, we consider a transmitter operating in hard saturation, i. e., a small change in voltage does not cause a change in the amplitude of the output. However, the electrical length of most transmitters changes if the operating voltage is perturbed. This phenomenon, known generically as pushing, causes phase modulation of the the output signal. Equation 5.1 shows the resultant perturbed chirp waveform which has been phase-modulated by a sinusoidal error voltage of frequency ν_i .

$$f(t) = \exp \left\{ j \left(\frac{\pi B t^2}{T} + \alpha \cos 2\pi \nu_i t \right) \right\} \quad (5.1)$$

The cosine term in the exponent can be expanded to give

$$f(t) = \exp \left\{ j \left(\frac{\pi B t^2}{T} \right) \right\} \sum_{k=-\infty}^{\infty} (j)^k J_k(\alpha) e^{jk2\pi \nu_i t} \quad (5.2)$$

where J_k is the Bessel function of the first kind of order k . For small values of the argument α , the time waveform can be expressed as

$$f(t) \approx \left(1 + j\alpha \cos 2\pi v_i t\right) \exp\left\{j\frac{\pi B t^2}{T}\right\} \quad (5.3)$$

After transformation of the waveform to the frequency domain, dechirping, and transforming back to the time domain, the compressed pulse, $F_c(t)$, has the form

$$F_c(t) = \text{sinc}\pi B t + j\frac{\alpha}{2} \left\{ \text{sinc}\pi B \left[t - \left(\frac{v_i T}{B} \right) \right] + \text{sinc}\pi B \left[t + \left(\frac{v_i T}{B} \right) \right] \right\} \quad (5.4)$$

The last two terms in equation 5.4 have their maxima offset from the main response at $t = 0$ by $t_s = \pm \left(\frac{v_i T}{B} \right)$, respectively. If t_s lies in the sidelobe region, then the sidelobe level will be perturbed. We compute the lower bound for the sidelobe interfering frequency $v_{i_{\min}}$, by requiring that t_s be greater than t_{01} the first zero of the weighted compressed time waveform. For Taylor weighting with $\bar{n} = 7$, SLL = 42 dB, the first zero occurs at $t_{01} = \frac{1.28}{B}$. Hence,

$$v_{i_{\min}} = \frac{1.28}{T} \quad (5.5)$$

which is independent of the signal bandwidth. In this case, coherent integration will not decrease the level of sidelobe perturbation since the magnitude of the principal signal and of the perturbing signals increase at the same rate.

The most common sphere used as a test target is satellite 5398, whose RCS is 1 square meter. Its circumference at the center frequency of the COBRA DANE high resolution waveform, 1.275 GHz, is 15.1 wavelengths. The creeping wave phenomenon is significant for this size sphere. The effect can be derived by studying the frequency variation of the RCS. Knott, Sheffer, and Tuley^[3] show that the radar-cross section of a sphere of radius a , as a function of wavelength λ , can be represented by the Mie series shown in equation 5.6.

$$\sigma = \frac{\lambda^2}{\pi} \left| \sum_{n=1}^{\infty} (-1)^n \left(n + \frac{1}{2}\right) (b_n - a_n) \right|^2 \quad (5.6)$$

The coefficients a_n and b_n are related to the spherical Bessel functions of ka by equations 5.7 and 5.8.

$$a_n = \frac{j_n(ka)}{h_n^{(1)}(ka)} \quad (5.7)$$

$$b_n = \frac{kaj_{n-1}(ka) - nj_n(ka)}{kjh_{n-1}^{(1)}(ka) - nh_n^{(1)}(ka)} \quad (5.8)$$

Equations 5.9, 5.10, and 5.11 show the relation between the spherical Bessel functions of order n and the Bessel functions of order $n + \frac{1}{2}$.

$$j_n(z) = \sqrt{\frac{\pi}{2z}} J_{n+\frac{1}{2}}(z) \quad (5.9)$$

$$y_n(z) = \sqrt{\frac{\pi}{2z}} Y_{n+\frac{1}{2}}(z) \quad (5.10)$$

$$h_n^{(1)}(z) = j_n(z) + iy_n(z) \quad (5.11)$$

Figure 5-1 is a plot of the computed radar cross section of satellite 5398 over the high resolution CDSM waveform bandwidth extending from 1175 to 1375 MHz.

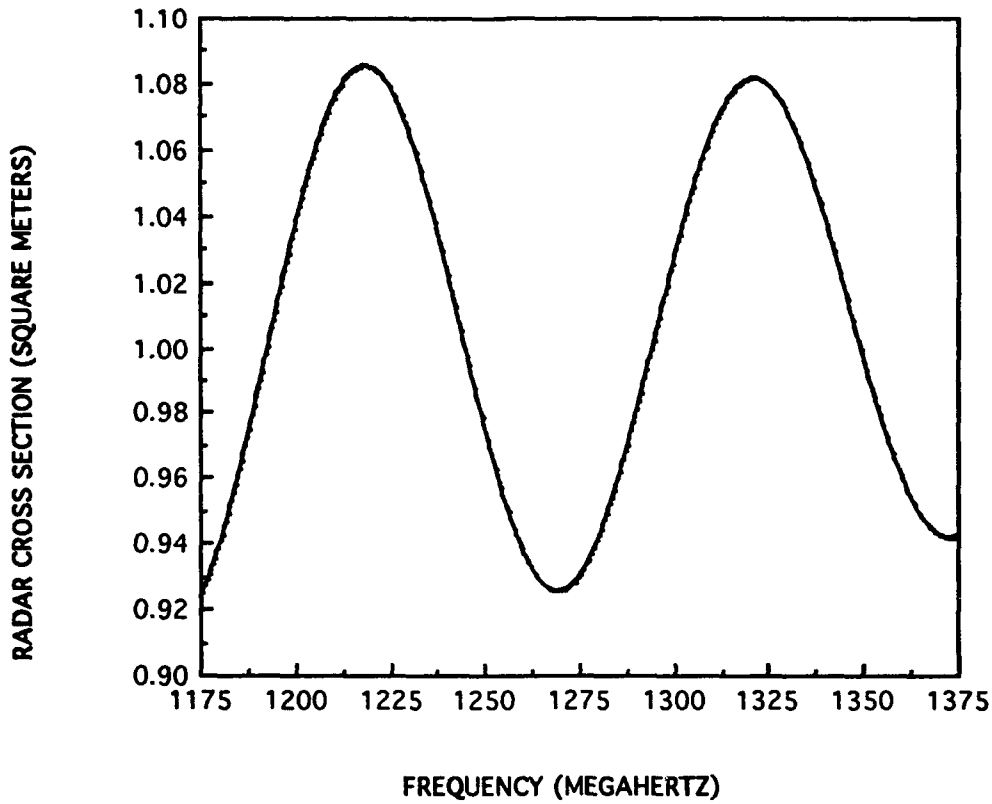


Figure 5-1. Radar Cross Section of 5398 in the High Resolution Operating CDSM Band

The radar cross section oscillates over the band with a period of $\Delta\nu \approx 103.3$ MHz. Over the operating band of the high resolution waveform, the curve in figure 5-1 can be approximated as

$$\sigma \approx 1 + 2\epsilon \cos\left(\frac{2\pi\nu}{\Delta\nu} + 1.305\right) \quad (5.12)$$

Indeed, σ can be approximated by

$$\sigma \approx \left| 1 + \epsilon \exp^{j(2\pi\nu\tau + 0.6525)} \right|^2 ; \tau = (\Delta\nu)^{-1} \quad (5.13)$$

The term within the absolute value brackets is the Fourier transform of the sum of a function of time, $f(t)$, and a delayed, smaller version of the same function, $\epsilon f(t + \tau)$.

This phenomena is due to a linear combination of a wave reflecting from the front of the sphere and a wave creeping around the sphere. Figure 5-2 illustrates the effect.

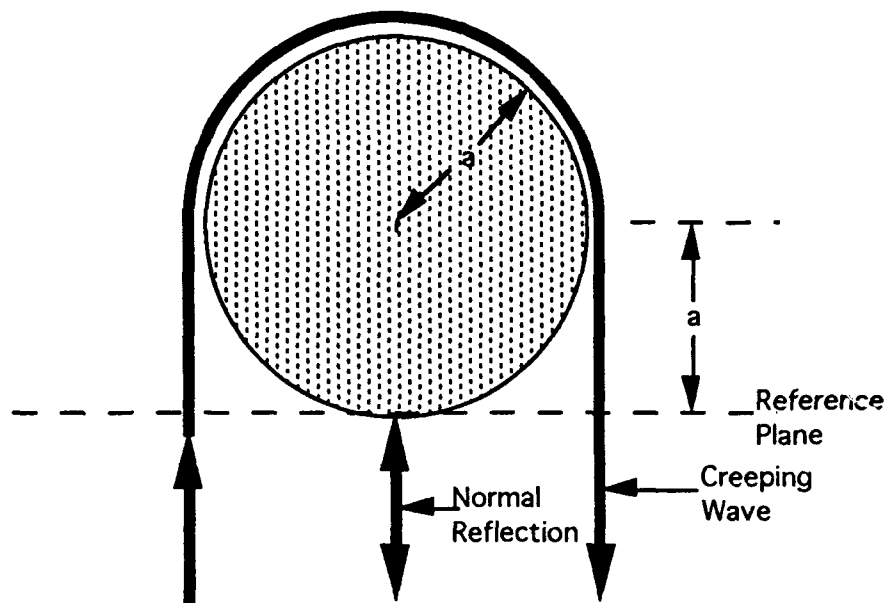


Figure 5-2. Schematic View of Reflection from a Conducting Sphere

The reference plane at the edge of the sphere of radius a is shown by the horizontal dashed line. A wave travels a distance equal to twice the radius a , plus one half of the circumference of the sphere, to return to the reference plane. This wave follows the path shown by the heavy line with arrows around the sphere. For a sphere of nominal radar cross section 1 square meter ($a = \pi^{-0.5}$ meters), the additional path length Δr is

$$(5.14) \quad \Delta r = a (2 + \pi) = \sqrt{2 + \pi} \sqrt{\pi}$$

Thus, the delay time, τ is

$$\tau = \frac{\Delta r}{c} = \frac{2 + \pi}{c \sqrt{\pi}} \quad (5.15)$$

For 5398 sphere, the value of τ is 9.7 nanoseconds.

The CDSM high resolution waveform (wideband) has a bandwidth of 200 MHz. The delay time τ is larger than the reciprocal of the wideband bandwidth. In this case, we expect to see a significant perturbation in the sidelobe region of the return. For the medium resolution CDSM waveform (narrowband) with an 8 MHz bandwidth, the reciprocal of the bandwidth is large compared to τ . In this case, we will not see a significantly perturbed return.

The time response of the pulse reflected from satellite 5398 is determined by adding the time response of the two signals. Figure 5-3 shows the time response of the reflection of the high resolution waveform from 5398, and the time response of the reflection of the same waveform from a sphere for which ka is very large.

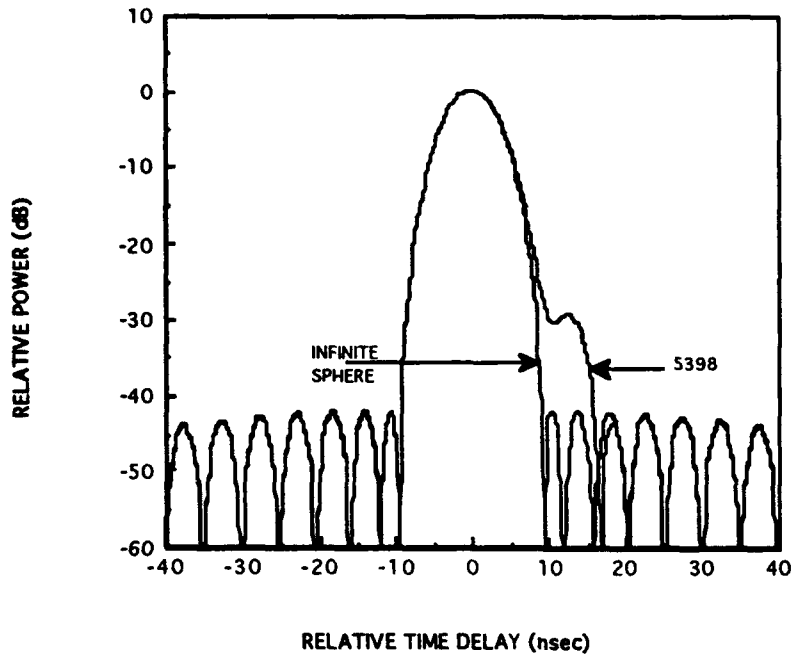


Figure 5-3. Time Waveforms

Figure 5-3 contains two curves. The curve marked "infinite sphere" is the reflected waveform response from a sphere for which $ka = \infty$. In this case, the amplitude of the creeping wave is of zero magnitude. The other curve, marked "5398", shows the L band response of the reflection from satellite 5398. The sidelobe level is asymmetrically raised significantly above the nominal level of 42 dB. The sidelobe maximum occurs at a time that corresponds to the previously computed quantity τ .

If satellite 5398 is used as a far field target for the measurement of range (or time) sidelobes of the high resolution waveform, the results are unacceptable. However, equalization networks can be used to reduce the effect of the creeping wave on the sidelobe structure for reflections from 5398. The consequent measurement, using 5398, shows an acceptable sidelobe level. However, reflections from other targets produce a high sidelobe level due to the effect of the equalization networks. We will call this effect "improper equalization".

As an example of the effect of improper equalization, we consider the effect of equalizing the creeping wave return from satellite 5398. The creeping wave from 5398 at L band is delayed by 9.67 nanoseconds and is of amplitude 0.04. Hence, it can be equalized using the network shown in figure 5-4.

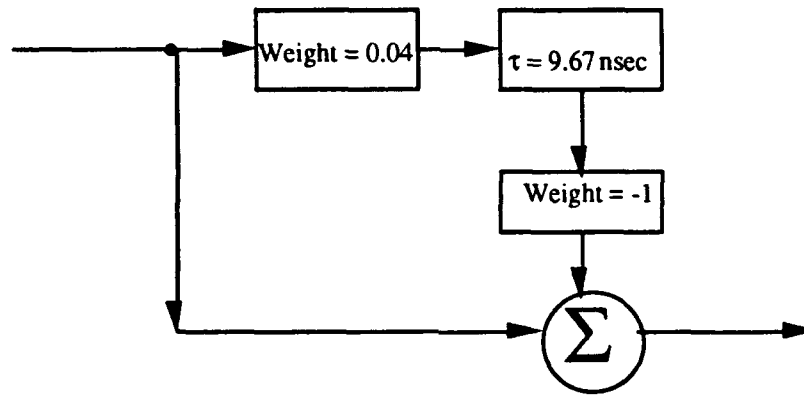


Figure 5-4. Equalization Network

When a large spherical target ($100 \leq ka$) reflects the improperly equalized wideband waveform, the compressed return waveform shows a high sidelobe lagging behind the main return. This phenomenon is shown in figure 5-5 as a solid line. For comparison, figure 5-5 shows the compressed, properly equalized waveform with a dashed line.

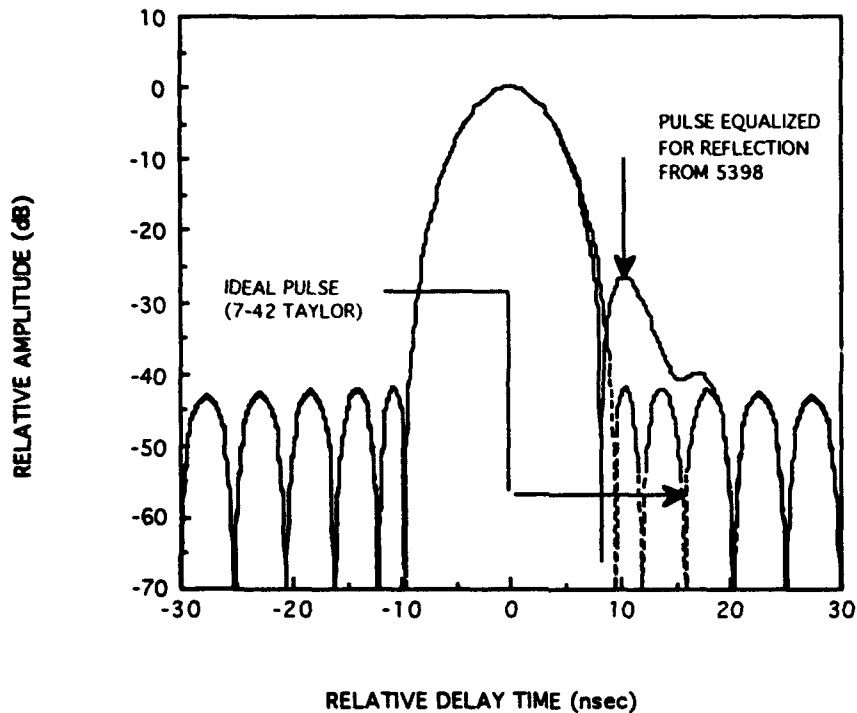


Figure 5-5. Equalized and Unequalized Waveforms

One can easily see the distortion in the improperly equalized return. The -27 dB lagging sidelobe looks like an additional return.

The major problem caused by equalization of the creeping wave sidelobe is the generation of false targets. We consider the compressed return from two real targets of equal magnitude that are separated in radial distance from the radar by 1.5 meters. The resultant return waveform is shown in figure 5-6 for the equalized and unequalized waveforms shown in figure 5-5.

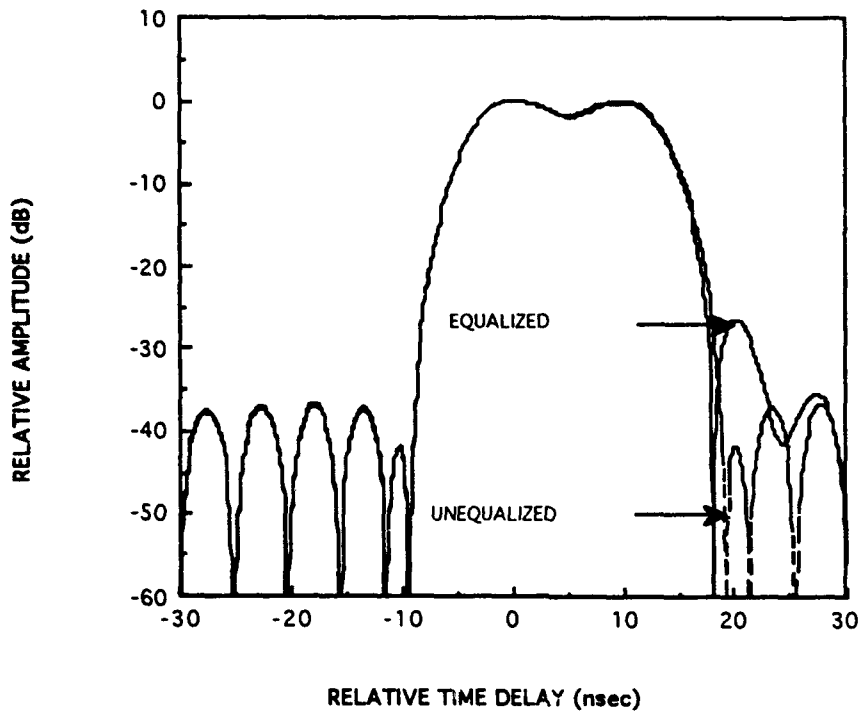


Figure 5-6. Radar Returns from Two Adjacent Targets

The solid curve is the expected return from the waveform, which is equalized to control the range sidelobe caused by the creeping wave around satellite 5398; the dashed curve is unequalized. Both curves show the presence of two equal resolved targets approximately 10 nanoseconds apart (1.5 meters). However, the solid curve shows the presence of a resolved target about 27 dB below either of the two main targets and delayed by about 9.7 nanoseconds from the lagging target (1.45 meters). Since this return is significantly greater than the expected range sidelobes, we must treat it as a real return without *a priori* knowledge of its presence. However, this return is spurious and its presence contaminates the data.

SECTION 6

CORRECT APPROACH

We can minimize the effects of the pathological problems described in Section 5 by proper design of the measurement procedure. If we know the etiology of the pathology, we can eliminate the source of the problem. For example, if the single pulse noise level is sufficiently high to obscure the lurking coherent errors, we can examine the Doppler sidelobes of the waveform to detect the existence of unwanted spectral lines. If we can identify the magnitude and frequency of the unwanted spectral lines, then we can equalize them. The resultant equalized waveform will show only those range sidelobes caused by incoherent effects.

We should not equalize creeping wave effects caused by the size of the sphere used for measurement. The magnitude of the amplitude of the creeping wave and the differential delay time from the target sphere are predictable if we know the magnitude of the optical radar-cross section ($\sigma_o = \pi a^2$ for a sphere of radius a). We can incorporate this recommendation in the test procedures and, to be safe, in the system specification and the operations and maintenance evaluation procedures. In this way, we minimize the acquisition of spurious data while monitoring the status of the system hardware.

SECTION 7

CONCLUSIONS

With sufficient care in test design, it is possible to provide a meaningful measurement of wideband and narrowband range sidelobes in the CDSM system. Integration effects can be minimized by using a large spherical target at close range and taking care to suppress coherent returns. Creeping wave effects cannot be avoided in the measurement. However, they must not be equalized.

LIST OF REFERENCES

1. Marcum, J. I. and P. Swerling, April 1960, "Studies of Target Detection by Pulsed Radar," IRE Transactions on Information Theory, *IT-6*, April 1960.
2. Marcum, J. I., January 1950, "Table of Q Functions," U. S. Air Force Project RAND Research Memorandum RM-339 (AD 116551).
3. Knott, E. F., J. F. Sheffer, and M. T. Tuley, 1985, "Radar Cross Section," Dedham, MA, Aertech House, Inc., pp. 88-90.
4. Taylor, T.T. , January 1955, "Design of Line-Source Antennas for Narrow Beamwidth and Low Side Lobes," I. R. E. J A&P, pp 16-28.

APPENDIX A

CALCULATION OF TAYLOR WEIGHTING COEFFICIENTS

The Taylor weighting is determined by the relationship

$$F_T(v) = \frac{1 + 2 \sum_{m=1}^{\bar{n}-1} F_m \cos \frac{2\pi m v}{B}}{\bar{n} - 1} \quad (A.1)$$

$$1 + 2 \sum_{m=1} F_m$$

where the weighting functions can be expressed in terms of the design sidelobe level (SLL, a negative number) and the number of "equal sidelobes" \bar{n} . Let

$$A = \frac{\cosh^{-1}(-0.05 \text{ SLL})}{\pi} \quad (A.2)$$

and let the quantity σ be defined from the relationship

$$\sigma^2 = \frac{\bar{n}^2}{A^2 + \left(\bar{n} - \frac{1}{2}\right)^2} \quad (A.3)$$

Then, Taylor^[4] shows that the coefficients F_m can be computed from the relationship

$$F_m = \frac{(-1)^{m+1} \prod_{n=1}^{\bar{n}-1} \left\{ 1 - \frac{m^2}{\sigma^2 \left[A^2 + \left(n - \frac{1}{2} \right)^2 \right]} \right\}}{2 \prod_{n=1}^{\bar{n}-1} \left\{ 1 - \left(\frac{m^2}{n^2} \right) \right\}} \quad (A.4)$$

(m ≠ n)